# PULSATILE BLOOD FLOW IN CONSTRICTED TAPERED ARTERY USING A VARIABLE-ORDER FRACTIONAL OLDROYD-B MODEL

by

***Hamzah BAKHTI*** [a*], ***Lahcen AZRAR*** [a,b], ***and Dumitru BALEANU*** [c,d]

[a] LaMIPI, Department of Mathematics, ENSET, Mohammed V University, Rabat, Morocco
[b] Department of Mechanical Engineering, Faculty of Engineering, KAU, Jeddah, Saudi Arabia
[c] Department of Mathematics, Cankaya University, Ankara, Turkey
[d] Institute of Space Sciences, Bucharest, Romania

Original scientific paper
DOI:10.2298/TSCI160421237B

*The aim of this paper is to deal with the pulsatile flow of blood in stenosed arteries using one of the known constitutive models that describe the viscoelasticity of blood witch is the generalized Oldroyd-B model with a variable-order fractional derivative. Numerical approximation for the axial velocity and wall shear stress were obtained by use of the implicit finite-difference scheme. The velocity profile is analyzed by graphical illustrations. This mathematical model gives more realistic results that will help medical practitioners and it has direct applications in the treatment of cardiovascular diseases.*

Key words: *blood flow, oldroyd-B, variable-order fractional derivative, stenosed tapered artery*

## Introduction

The non-Newtonian fluids give more realistic behavior of real and biological fluids and they are appropriate in technological applications because of it viscosity that does not follow the relation between viscous stress and rate of change witch is linear for the case of a Newtonian fluid. The non-linear dependence makes the study of the fluid flow becomes more complicated and not like the Newtonian fluids.

In the previous researches there are large number of studies involving Newtonian fluids leading to closed form analytical solutions. But, for non-Newtonian fluids it is quite hard to obtain exact solutions. Many researches are denoted to study blood flow in arteries with the consideration that blood behaves as Newtonian or non-Newtonian fluids and in many cases blood behaves as a non-Newtonian fluid especially at low shear rate. The Oldroyd-B model, introduced by Oldroyd [1, 2], is one of the simplest constitutive model that describes the flow of viscoelastic fluids especially polymer and biological liquids. Some of the interesting Oldroyd-B fluid flows are presented in [3-6]. Recently, Shahid *et al*. [7] examined the flow of an Oldroyd-B fluid over an infinite flat plate.

Fractional derivatives have been known for a long time ago, and they had a real success in describing some complex dynamics and the rheological properties of many types of fluids with more clear and deep understanding of its behavior by just substituting the time ordinary derivatives in the constitutive equations by derivatives of fractional order. Various work

* Corresponding author, e-mail: bakhti_hamzah@outlook.com

are made in this subject, as presented in [8-10]. This type of calculus allows defining precisely non-integer order derivatives or integrals. Some recent work on the fluid flows with fractional derivative models can be found in [11-15]. More recently, some results using alternative analytical approach to solve some problems with second order fluid can be found in [16, 17].

More recently, many researchers proposed an extension to the known constant-order (CO) fractional derivatives to variable-order (VO) witch gives more realistic results than the usual derivative or the CO fractional derivative in the description of the complex dynamics. In particular it has been found to be quite flexible in describing viscoelastic behavior. In general, these constitutive equations are derived from known models via substituting time ordinary derivatives of stress and strain by derivatives of fractional order. The original work of VO operator may be wrote by Samko and Ross [18, 19] witch gave the introduction to the VO integration. It has been known as a great way in the field of modeling real problems in many fields [20-22]. Some procedures are elaborated to find exact or numerical solution to such complex derivative [23, 24]. More references on VO fractional models are cited, for VO fractional diffusion model [25], difference between VO and constant order models [26].

For the moment, investigating the VO differential equations numerically is easy and more practical instead of searching for an analytical solution, witch are hard to obtain for some complex equations. Zhuang *et al*. [27] studied numerically VO fractional equations using finite difference schemes, the explicit scheme for VO fractional non-linear diffusion equation have been investigated by Lin *et al*. [28] and more recently Sun *et al*. [29] studied different numerical schemes for VO time-fractional diffusion equations.

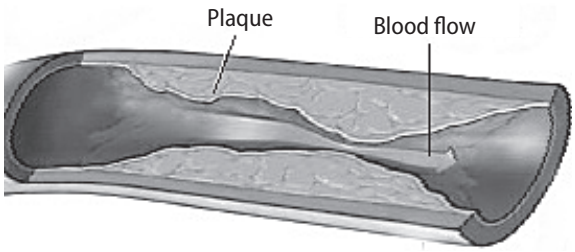


**Figure 1. Atherosclerosis is the buildup of fatty materials that can damage and clot arteries witch lead to constrict blood flow**

The study of blood flow through different types of arteries and different shapes of the stenosis is important in understanding of many cardiovascular diseases, one of them is atherosclerosis, fig. 1. In reality many geometries of vessels can be considered as long, narrow, and tapering cones. Akbar *et al*. [30] analyzed the effects of vessel tapering together with the asymmetric stenosed tapered artery on the flow by considering blood as a nanofluid. Also the stenosis may grow up in series manner, overlap with each other and it would be appear like $\omega$-shape. Srivastava and Mishra [31] explored the arterial blood flow through an overlapping stenosis by treating the blood as a Casson fluid. More recently Bakhti and Azrar [32] have analyzed the effects of asymmetric stenosed tapered artery on the flow using the Couple-Stress fluid.

In this paper a mathematical model for the pulsatile blood flow through tapered stenosed artery due to pressure gradient is presented by considering blood as a VO fractional Oldroyd-B fluid in a circular tube. The motivation is to give more realistic understanding of the blood flow in stenosed arteries using fractional calculus. The main aim of this work is to study numerically these phenomena and give numerical illustrations of the axial velocity as well as to study the effect of different fluid and geometry parameters on the flow. Results for the Oldroyd-B, VO fractional Maxwell, ordinary Maxwell fluids, and Newtonian fluids are obtained as limiting cases for different values of the model parameters.

## Problem formulation

A mathematical model is elaborated for unidirectional pulsatile blood flow through a rigid tapered stenosed artery by considering blood as an incompressible as on the generalized Oldroyd-B fluid with VO fractional derivatives. The geometry of the tapered stenosed artery is shown in figs. 2(a) and 2(b), and can be expressed mathematically as [32]:

$$R(z)=\begin{cases}(R_0+\zeta z)\left\{1-\dfrac{\epsilon n^{n/(n-1)}}{(n-1)L_0^n}\left[L_0^{n-1}(z-d)-(z-d)^n\right]\right\}, & d\le z\le d+L_0\\ R_0+\zeta z, \quad \text{otherwise}\end{cases} \tag{1}$$

where $R_0$ is the radius of the non-tapered and healthy region of the artery, $n$ – the shape of the stenosis, $L_0$ – the stenosis length, $d$ – the location of stenosis, $\epsilon$ – the maximum height of the stenosis, $\zeta=\tan\phi$ – the tapering parameter which represents the slope of the tapered vessel with the tapering angle, $\phi$, $\phi<0$, $\phi>0$, and $\phi=0$ are for converging, diverging, and non-tapering artery, respectively.

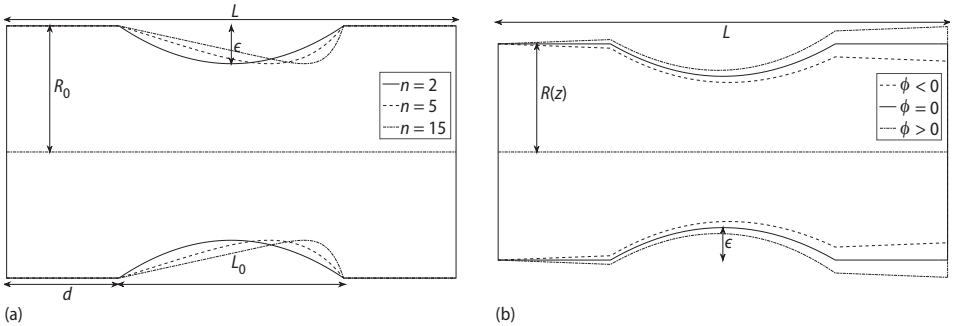


**Figure 2. The 2-D view of a stenosed (a) tapered (b) artery**

An incompressible generalized Oldroyd-B fluid with VO derivative is characterized by the following constitutive equations [12, 13]:

$$\mathbf{T}=-p\mathbf{I}+\mathbf{S},\quad \mathbf{S}+\lambda\left(D_t^{\alpha(x,t)}\mathbf{S}-\mathbf{LS}-\mathbf{SL}^T\right)=\mu\left[\mathbf{A}+\lambda_r\left(D_t^{\beta(x,t)}\mathbf{A}-\mathbf{LA}-\mathbf{AL}^T\right)\right] \tag{2}$$

where $\mathbf{T}$ presents the Cauchy stress tensor, $p$ – the pressure, $S$ – the extra-shear stress tensor, $\mathbf{L}=\nabla\vec{\mathrm{V}}$ – the velocity gradient where $\vec{\mathrm{V}}$ being the velocity vector, $\mathbf{A}=\mathbf{L}+\mathbf{L}^T$ – the first Rivlin-Ericksen tensor, $\mu$ – the viscosity of the fluid, and $\lambda$ and $\lambda_r$ are the relaxation and retardation times, respectively. The superscript $T$ indicates the transpose operation and $D_t^{\alpha(x,t)}$, $D_t^{\beta(x,t)}$ denote the VO (in time, $t$, and space, $x$) fractional time-derivatives in Caputo's sense, which is defined [20]:

$$D_t^{\alpha(t)}f(t)=\frac{1}{\Gamma\left[n-\alpha(t)\right]}\int_0^t\frac{f'(\tau)}{(t-\tau)^{\alpha(t)}}\mathrm{d}\tau,\quad 0<\alpha(t)<1 \tag{3}$$

where $\Gamma(\bullet)$ is the gamma function. This VO fractional derivative reduces to the local derivative when $\alpha=1$ because $D_t^1 f=\mathrm{d}f/\mathrm{d}t$.

The conservation equations which govern the Oldroyd-B fluid flow can be written:

$$\nabla\cdot\vec{\mathrm{V}}=0 \tag{4}$$

$$\rho\frac{\mathrm{d}\vec{\mathrm{V}}}{\mathrm{d}t}=\nabla\cdot\mathbf{T}+\rho\vec{\mathrm{b}} \tag{5}$$

where $\rho$ denotes the density, $\vec{b}$ – the body accelerations field, d/d$t$ – the material time differentiation, and $\nabla$ – the divergence operator.

In the following analysis, we suppose that the flow is in the z-axis direction so the velocity field and stress are of the form:

$$\vec{V} = \vec{V}(r,t) = w(r,t)\vec{e}_z, \quad \mathbf{S} = \tau_{RZ}(r,t)\vec{e}_z \tag{6}$$

where $\vec{e}_z$ and $w$ are the unit vectors and velocity in the z-direction, respectively, $\tau_{RZ}$ – the shear stress tensor acting on the r-plane toward the z-direction.

The pressure gradient $\partial p/\partial z$, produced by the pumping action of the heart, is given by:

$$-\frac{\partial p}{\partial z} = k_s + k_\phi \cos(\omega_p t) \tag{7}$$

where $k_s$ is the steady part of the pressure gradient, $k_\phi$ – the amplitude of the oscillatory part, and $\omega_p = 2\pi f_p$, where $f_p$ is the heart pulse frequency.

The continuity equation is satisfied when we substitute eq. (6) into eq. (4), while the substitution into eqs. (2) and (5) gives us the following equations:

$$\left(1 + \lambda D_t^{\alpha(r,t)}\right)\tau = \mu\left(1 + \lambda_r D_t^{\beta(r,t)}\right)\frac{\partial w}{\partial r} \tag{8}$$

$$\rho\frac{\partial w}{\partial t} = -\frac{\partial p}{\partial z} + \left(\frac{\partial}{\partial r} + \frac{1}{r}\right)\tau \tag{9}$$

Eliminating $\tau$ between the two equations, leads to the following governing equation:

$$\rho\left[1 + \lambda D_t^{\alpha(r,t)}\right]\frac{\partial w}{\partial t} = -\left[1 + \lambda D_t^{\alpha(r,t)}\right]\frac{\partial p}{\partial z} + \mu\left[1 + \lambda_r D_t^{\beta(r,t)}\right]\left(\frac{\partial^2}{\partial r^2} + \frac{1}{r}\frac{\partial}{\partial r}\right)w \tag{10}$$

The following dimensionless quantities are introduced:

$$\begin{aligned} &r^* = \frac{r}{R_0}, \quad z^* = \frac{z}{L_0}, \quad t^* = \omega t, \quad \epsilon^* = \frac{\epsilon}{R_0}, \\ &\zeta^* = \frac{\zeta L_0}{R_0}, \quad \lambda^* = \omega\lambda, \quad \lambda_r = \omega\lambda_r, \\ &k_s^* = \frac{R^2}{\mu L_0}k_s, \quad k_\theta^* = \frac{R^2}{\mu L_0}k_\theta, \quad p^* = \frac{R^2}{\mu L_0}p \end{aligned} \tag{11}$$

The dimensionless form of the geometry (1) after dropping the stars is thus obtained:

$$R(z) = \begin{cases} (1+\zeta z)\left\{1 - \dfrac{\zeta n^{n/(n-1)}}{n-1}\left[(z-\gamma) - (z-\gamma)^n\right]\right\}, & \gamma \le z \le \gamma + 1 \\ 1 + \zeta z, \quad \text{otherwise} \end{cases} \tag{12}$$

where $\gamma = L_0/L_1$, and $w_0$ is a typical axial velocity.

Also, eq. (10), after dropping the stars, becomes:

$$\bar{\alpha}^2\left[1 + \lambda D_t^{\alpha(r,t)}\right]\frac{\partial w}{\partial t} = \left[1 + \lambda D_t^{\alpha(r,t)}\right]\left[k_s + k_\theta \cos(bt)\right] + \left[1 + \lambda_r D_t^{\beta(r,t)}\right]\left(\frac{\partial^2}{\partial r^2} + \frac{1}{r}\frac{\partial}{\partial r}\right)w \tag{13}$$

where $\overline{\alpha}^2 = R_0^2(\omega\rho/\mu)$ is Womersley parameter.

The corresponding non-dimensional initial and boundary conditions are:

$$\begin{cases} \tau_{\mathrm{RZ}}(r,0)=0 \\ w(r,t)=\dfrac{\partial w}{\partial t}(r,t)\to 0 \text{ as } t\to 0 \\ w=0 \text{ at } r=R(z) \\ w \text{ is finite at } r=0 \end{cases} \tag{14}$$

## Numerical approximations

The implicit finite-difference scheme is applied to the problem (10) alongside with the initial and boundary conditions (14). Before that, let suppose that eq. (10) has a unique and smooth solution. Now, let $r_i = i\Delta r$, $0 \le i \le M$, $M\Delta r = R$ and $t_n = n\Delta t$, $0 \le n \le N$, $N\Delta t = T$, where $\Delta r$ is the radial step and $\Delta t$ is the time step, also $M$ and $N$ are grid points, we suppose that $w_i^n \simeq w(r_i, t_n)$.

The first and second derivative are classically approximated by the implicit finite difference equations:

$$\frac{\partial^2 w}{\partial r^2}(r_i,t_{n+1}) \simeq \frac{w_{i+1}^{n+1} - 2w_i^{n+1} + w_{i-1}^{n+1}}{\Delta r^2} \tag{15}$$

$$\frac{\partial w}{\partial r}(r_i,t_{n+1}) \simeq \frac{w_{i+1}^{n+1} - w_i^{n+1}}{\Delta r} \tag{16}$$

The discretization of the VO fractional derivative is given [27]:

$$D_t^{\alpha_i^{n+1}} w(r_i,t_{n+1}) \simeq \frac{\Delta t^{-\alpha_i^{n+1}}}{\Gamma\left(2-\alpha_i^{n+1}\right)}\left\{ w_i^{n+1} - w_i^n + \sum_{k=1}^{n}\left(w_i^{n+1-k} - w_i^{n-k}\right)\left[\left(k+1\right)^{1-\alpha_i^{n+1}} - k^{1-\alpha_i^{n+1}}\right]\right\} \tag{17}$$

Therefore, the implicit scheme of the problem can be written:

$$\begin{aligned} &\frac{\overline{\alpha}^2}{\Delta t}\left\{ w_i^{n+1} - w_i^n + \nu_i^{n+1}\left[ w_i^{n+1} - 2w_i^n + w_i^{n-1} + \sum_{k=1}^{n}\left(w_i^{n+1-k} - 2w_i^{n-k} + w_i^{n-k-1}\right)c_k^{i,n+1}\right]\right\} = \\ &= \left\{ f^{n+1} + \nu_i^{n+1}\left[ f^{n+1} - f^n + \sum_{k=1}^{n}\left(f^{n+1-k} - f^{n-k}\right)c_k^{i,n+1}\right]\right\} + \left\{ \frac{w_{i+1}^{n+1} - 2w_i^{n+1} + w_{i-1}^{n+1}}{\Delta r^2} + \right. \\ &+ \frac{1}{r_i}\frac{w_{i+1}^{n+1} - w_i^{n+1}}{\Delta r} + \eta_i^{n+1}\left[ \frac{w_{i+1}^{n+1} - 2w_i^{n+1} + w_{i-1}^{n+1}}{\Delta r^2} + \frac{1}{r_i}\frac{w_{i+1}^{n+1} - w_i^{n+1}}{\Delta r} - \frac{w_{i+1}^{n} - 2w_i^{n} + w_{i-1}^{n}}{\Delta r^2} + \right. \\ &\left. + \frac{1}{r_i}\frac{w_{i+1}^{n} - w_i^{n}}{\Delta r} + \sum_{k=1}^{n}\left( \frac{w_{i+1}^{n+1-k} - 2w_i^{n+1-k} + w_{i-1}^{n+1-k}}{\Delta r^2} + \frac{1}{r_i}\frac{w_{i+1}^{n+1-k} - w_i^{n+1-k}}{\Delta r} - \right.\right. \\ &\left.\left. \left. - \frac{w_{i+1}^{n-k} - 2w_i^{n-k} + w_{i-1}^{n-k}}{\Delta r^2} + \frac{1}{r_i}\frac{w_{i+1}^{n-k} - w_i^{n-k}}{\Delta r}\right) d_k^{i,n+1}\right]\right\} \end{aligned} \tag{18}$$

where

$$v_i^{n+1}=\lambda\frac{\Delta t^{-\alpha_i^{n+1}}}{\Gamma\left(2-\alpha_i^{n+1}\right)},\quad \nu_i^{n+1}=\lambda_r\frac{\Delta t^{-\beta_i^{n+1}}}{\Gamma\left(2-\beta_i^{n+1}\right)},\quad c_k^{i,n+1}=\left(k+1\right)^{1-\alpha_i^{n+1}}-k^{1-\alpha_i^{n+1}},$$

$$d_k^{i,n+1}=\left(k+1\right)^{1-\beta_i^{n+1}}-k^{1-\beta_i^{n+1}},\quad f^{n+t}=k_s+k_\theta\cos\left(bt_{n+1}\right),\ i=1,2,\cdots,M-1\quad\text{and}\quad n=1,2,\cdots,N$$

For the boundary and initial conditions:

$$\begin{cases} w_i^0=w_i^1=0, & i=0,2,\cdots,M\\ w_M^n=0, & n=0,1,2,\cdots,N+1\\ w_1^n=w_0^n, & n=0,1,2,\cdots,N+1\end{cases}\tag{19}$$

It should be pointed out that the sum terms automatically vanishes when $n = 0$. Equation (18) can be transferred into the following matrix form:

$$\begin{aligned}&W^0=W^1=0,\\&\left(\frac{\bar{\alpha}^2}{\Delta t}\left(\left[\mathrm{I}\right]+\left[\nu^{n+1}\right]\right)-\left(\left[\mathrm{I}\right]-\left[\eta^{n+1}\right]\right)\left[\mathrm{A}\right]\right)W^{n+1}=\\&=\left(\frac{\bar{\alpha}^2}{\Delta t}\left(\left[\mathrm{I}\right]-2\left[\nu^{n+1}\right]\right)-\left[\eta^{n+1}\right]\left[\mathrm{A}\right]\right)W^n-\frac{\bar{\alpha}^2}{\Delta t}\left[\nu^{n+1}\right]W^{n-1}+\\&+\left[\eta^{n+1}\right]\sum_{k=1}^{n}\left[D_k^{n+1}\right]\left(\left[\mathrm{A}\right]W^{n+1-k}-\left[\mathrm{A}\right]W^{n-k}\right)-\\&-\frac{\bar{\alpha}^2}{\Delta t}\left[\nu^{n+1}\right]\sum_{k=1}^{n}\left[C_k^{n+1}\right]\left(W^{n+1-k}-2W^{n-k}+W^{n-k-1}\right)+\\&+F^{n+1}+\left[\nu^{n+1}\right]\left\{F^{n+1}-F^n+\sum_{k=1}^{n}\left[C_k^{n+1}\right]\left(F^{n+1-k}-F^{n-k}\right)\right\}\end{aligned}\tag{20}$$

where

$$\left[\mathrm{A}\right]=\left[\mathrm{A}_1\right]+\left[\mathrm{A}_2\right]\tag{21}$$

$$\left[\mathrm{A}_1\right]=\frac{1}{\Delta r^2}\begin{bmatrix}-1&1&0&\cdots&0\\1&-2&1&\ddots&\vdots\\0&\ddots&\ddots&\ddots&0\\\vdots&\ddots&1&-2&1\\0&\cdots&0&-1&-2\end{bmatrix}$$

$$\left[\mathrm{A}_2\right]=\frac{1}{\Delta r}\begin{bmatrix}-1/r_1&1/r_1&0&\cdots&0\\0&-1/r_2&1/r_2&\ddots&\vdots\\\vdots&\ddots&\ddots&\ddots&0\\\vdots&\ddots&\ddots&-1/r_{M-2}&1/r_{M-2}\\0&\cdots&\cdots&0&-1/r_{M-1}\end{bmatrix}\tag{22}$$

$$\left[\nu^{n+1}\right]=\lambda\mathrm{diag}\begin{bmatrix}\dfrac{\Delta t^{-\alpha_1^{n+1}}}{\Gamma\left(2-\alpha_1^{n+1}\right)}\\ \vdots\\ \dfrac{\Delta t^{-\alpha_{M-1}^{n+1}}}{\Gamma\left(2-\alpha_{M-1}^{n+1}\right)}\end{bmatrix},\quad \left[\eta^{n+1}\right]=\lambda_r\mathrm{diag}\begin{bmatrix}\dfrac{\Delta t^{-\beta_1^{n+1}}}{\Gamma\left(2-\beta_1^{n+1}\right)}\\ \vdots\\ \dfrac{\Delta t^{-\beta_{M-1}^{n+1}}}{\Gamma\left(2-\beta_{M-1}^{n+1}\right)}\end{bmatrix} \tag{23}$$

$$W^{n+1}=\begin{pmatrix}w_1^{n+1}\\ \vdots\\ w_{M-1}^{n+1}\end{pmatrix},\quad F^{n+1}=f^{n+1}\begin{pmatrix}1\\ \vdots\\ 1\end{pmatrix} \tag{24}$$

$$\left[D_k^{n+1}\right]=\mathrm{diag}\begin{bmatrix}d_k^{1,n+1}\\ \vdots\\ d_k^{M-1,n+1}\end{bmatrix},\quad \left[C_k^{n+1}\right]=\mathrm{diag}\begin{bmatrix}c_k^{1,n+1}\\ \vdots\\ c_k^{M-1,n+1}\end{bmatrix} \tag{25}$$

and [I] is the identity matrix of dimensions (M–1)×(M–1). Using the same process for shear stress, the implicit scheme of eq. (8), is given by:

$$\begin{aligned}&\left\{\tau_i^{n+1}+\nu_i^{n+1}\left[\tau_i^{n+1}-\tau_i^n+\sum_{k=1}^{n}\left(\tau_i^{n+1-k}-\tau_i^{n-k}\right)c_k^{i,n+1}\right]\right\}=\frac{1}{\Delta r}\left\{\frac{w_{i+1}^{n+1}-w_i^{n+1}}{\Delta r}+\right.\\&\left.+\eta_i^{n+1}\left[w_{i+1}^{n+1}-w_i^{n+1}+w_{i+1}^{n}-w_i^{n}+\sum_{k=1}^{n}\left(w_{i+1}^{n+1-k}-w_i^{n+1-k}-w_{i+1}^{n-k}-w_i^{n-k}\right)d_k^{i,n+1}\right]\right\}\end{aligned} \tag{26}$$

Equation (26) can be transferred into a matrix form:

$$\begin{aligned}&\bar{\tau}^0=0\\&\left(\left[\mathrm{I}\right]+\left[\nu^{n+1}\right]\right)\bar{\tau}^{n+1}=\left[\nu^{n+1}\right]\bar{\tau}^n-\left[\nu^{n+1}\right]\sum_{k=1}^{n}\left[C_k^{n+1}\right]\left(\bar{\tau}^{n+1-k}-\bar{\tau}^{n-k}\right)+\\&+\frac{1}{\Delta r}\left\{\left(\left[\mathrm{I}\right]+\left[\eta^{n+1}\right]\left[\mathrm{A}_2\right]\right)W^{n+1}-\left[\eta^{n+1}\right]\left[\mathrm{A}_2\right]W^n+\right.\\&\left.+\left[\eta^{n+1}\right]\sum_{k=1}^{n}\left[D_k^{n+1}\right]\left(\left[\mathrm{A}_2\right]W^{n+1-k}-\left[\mathrm{A}_2\right]W^{n-k}\right)\right\}\end{aligned} \tag{27}$$

where

$$\bar{\tau}^{n+1}=\begin{pmatrix}\tau_1^{n+1}\\ \vdots\\ \tau_{M-1}^{n+1}\end{pmatrix} \tag{28}$$

The presented methodological approach allows investigating the velocity field $w(r,t)$ corresponding to the pulsatile flow in a tapered stenosed artery using the generalized Oldroyd-B model with VO fractional derivative where the flow is due to pressure gradient. The model as well as material and geometrical parameters effects on the velocity field can be easily analyzed. Other models such as Maxwell and second grade fluids can be resulted as special cases of the presented approach.

## Results and discussion

Let us consider a stensed tapered arteries, presented in fig. (2), with the following parameters: $d = 0.5$, $L_0 = 1$, $L = 2$, $n = 5$, $k_s = 0.8$, $k_\theta = 0.1$, and $b = 0.5$.

We suppose that the VO fractional derivatives $\alpha$ and $\beta$ are given by:

$$\alpha(r,t) = 0.5 + 0.4\cos\left(\pi\frac{r}{R}\right) + 0.1t \tag{29}$$

$$\beta(r,t) = 0.1 + 0.05\cos\left(\pi\frac{r}{R}\right) + 0.1t^2 \tag{30}$$

In order to reveal some relevant physical aspects of the obtained results, the diagrams of the velocity profiles $w(r,t)$ are depicted against $r$. The effects of various geometric parameters and the parameters arising out of the fluid model are discussed. The parameters considered are tapered parameter, $\zeta$, the height of the stenosis, $\epsilon$, relaxation time, $\lambda$, the retardation time, $\lambda_r$, Womersley number, $\overline{\alpha}$, and time, $t$.

Figures 3 and 4 illustrate the variation of axial velocity profile for different values of $\zeta$ and $\epsilon$, respectively. It is observed from fig. 3, that the velocity increases by the increase in the tapered parameter, $\zeta$, and from fig. 4 that the velocity profile decreases for increasing the height of the stenosis because of the obstruction to the flow.

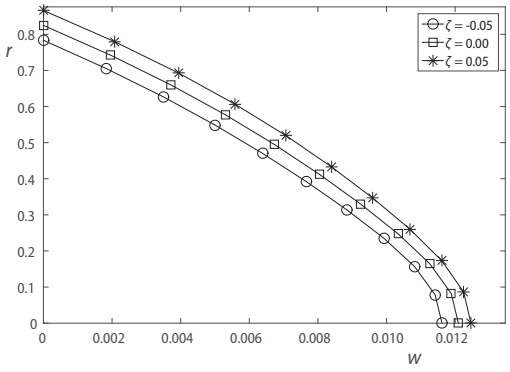


**Figure 3. Variation of axial velocity $w$ with respect to $\zeta$ when $\epsilon = 0.2$, $\lambda = 15$, $\lambda_r = 10$, $\overline{\alpha} = 2$, and $t = 0.8$**

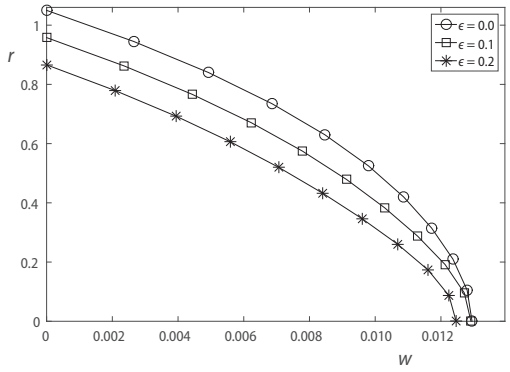


**Figure 4. Variation of axial velocity $w$ with respect to $\epsilon$ when $\zeta = 0.05$, $\lambda = 15$, $\lambda_r = 10$, $\overline{\alpha} = 2$, and $t = 0.8$**

The effect of the relaxation time, $\lambda$, on the fluid flow is shown in fig. 5 in which the velocity is a decreasing function of the relaxation time. On the other hand, the influence of the retardation time, $\lambda_r$, is shown in fig. 6 in which the velocity is also a decreasing function of the retardation time.

Figures 7 and 8 show the variation of the velocity profile with respect to Womersley parameter, $\alpha$, and time, $t$, respectively. It can be seen that $w(r,t)$ is decreasing (resp. increasing) function of Womersley parameter $\alpha$ (resp. time $t$).

It is observed from experimental data that the peak value of the velocity does not always appears in the middle of the artery (symmetry axis) but for some cases the peak velocity can be near the artery wall (between the center of the artery and the wall). Thus, the use of the VO (in space and time) fractional derivative in fluid models can give us more realistic results than the usual derivative or the CO fractional derivative as also observed from experimental results [33, 34].

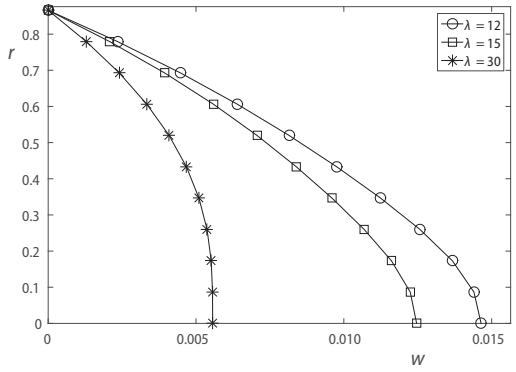


**Figure 5. Variation of axial velocity $w$ with respect to $\lambda$ when $\zeta = 0.05$, $\epsilon = 0.2$, $\lambda_r = 10$, $\overline{\alpha} = 2$, and $t = 0.8$**

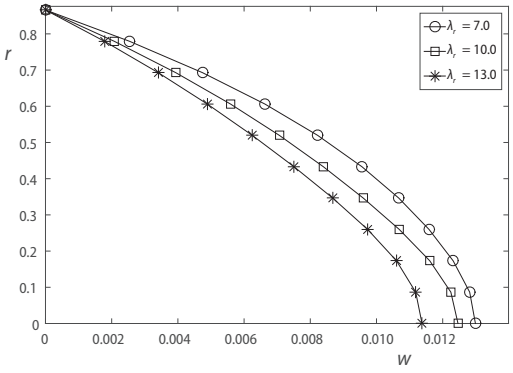


**Figure 6. Variation of axial velocity $w$ with respect to $\lambda_r$ when $\zeta = 0.05$, $\epsilon = 0.2$, $\lambda = 15$, $\overline{\alpha} = 2$, and $t = 0.8$**

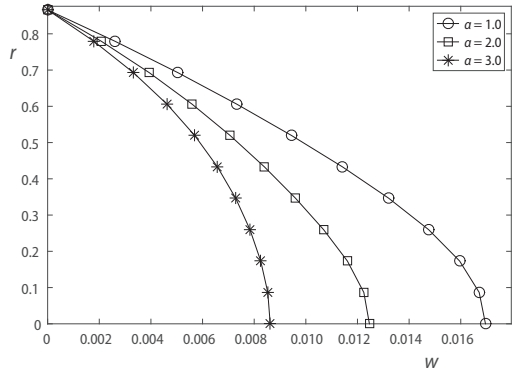


**Figure 7. Variation of axial velocity $w$ with respect to $\alpha$ when $\zeta = 0.05$, $\epsilon = 0.2$, $\lambda = 15$, $\lambda_r = 10$, and $t = 0.8$**

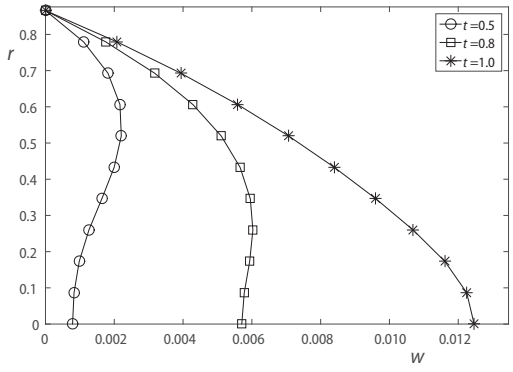


**Figure 8. Variation of axial velocity $w$ with respect to $t$ when $\zeta = 0.05$, $\epsilon = 0.2$, $\lambda = 15$, $\lambda_r = 10$, and $\overline{\alpha} = 2$**

As a comparison, the obtained results of $w(r,t)$ based on the VO fractional models corresponding to Oldroyd-B, Maxwell, and second grade fluids are plotted in fig. 9 for fixed values of material parameters and time. It is observed that the peak value of the velocity appears in middle of the artery (symmetry axis) for the Oldroyd-B and second grade fluids, while for Maxwell fluid the peak velocity appears near the artery wall. Moreover, in the middle of the artery the second grade fluid is the swiftest. Also, near the artery wall, the Maxwell fluid appears to be the fastest and Oldroyd-B fluid is the slowest.

Based on the presented model, various kinds of fractional derivatives can be used and the resulted profile $w(r,t)$ can be obtained. The velocity profile $w(r,t)$ can take several forms when we use different types of fractional models as shown in fig. 10. For these results we take VO (in time and space) fractional derivative VO – $\alpha(r,t) = 0.5 + 0.4\cos(\pi r/R) + 0.1t$ and $\beta(r,t) = 0.1 + 0.05\cos(\pi r/R) + 0.1t^2$, time-order (TO) fractional derivative – $\alpha(r, t) = 0.6 + 0.1t$ and $\beta(r, t) = 0.2 + 0.1t^2$, CO fractional derivative – $\alpha(r,t) = 0.6$ and $\beta(r,t) = 0.2$.

The numerical computations show that the solutions, obtained by use of the implicit finite-difference scheme and presented graphically, satisfy the imposed initial and boundary conditions. Also, we can obtain the solutions corresponding to Maxwell fluids and second grade fluids by taking $\lambda_r \to 0$ or $\lambda \to 0$, respectively.

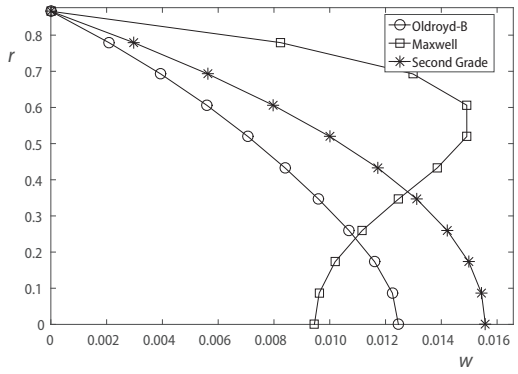


**Figure 9. Axial velocity *w* for Oldroyd-B, Maxwell, and second grade fluids with VO fractional derivative when $\zeta = 0.05$, $\epsilon = 0.2$, $\lambda = 15$, $\lambda_r = 10$, $\overline{\alpha} = 2$, and $t = 0.8$**

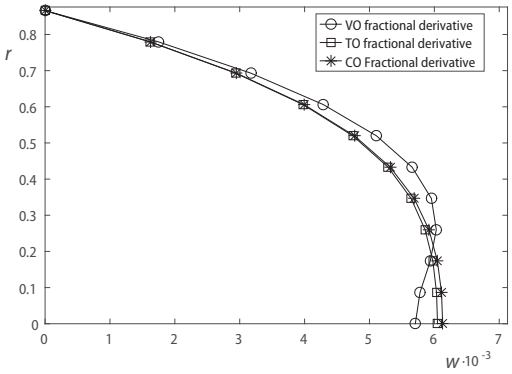


**Figures 10. Axial velocity *w* for VO, time-variable, and CO fractional derivative when $\zeta = 0.05$, $\epsilon = 0.2$, $\lambda = 15$, $\lambda_r = 10$, $\overline{\alpha} = 2$, and $t = 0.8$**

## Conclusions

A mathematical model has been elaborated to investigate the pulsatile flow of blood through an asymmetric tapered stenosed artery due to pressure gradient using the generalized Oldroyd-B with VO fractional derivative. The implicit finite difference approach combined with a VO fractional discretization approach is elaborated. A matrix formulation is presented allowing to take into account various types of VO fractional derivative parameters as well as various geometrical parameters. Numerical solutions are obtained and the effects of various geometric and fluid parameters on the axial velocity of the blood are studied.

Generalized Oldroyd-B fluid can be regarded as an extension of the Maxwell and second grade fluid. Also when $\lambda = 0$ and $\lambda_r = 0$, we obtain the Newtonian fluid. When $\lambda_r = 0$, we obtain the Maxwell fluid and when $\lambda = 0$, we have the second grade fluid. As previously mentioned a numerical scheme was followed to solve the mathematical model of blood flow through stenosed tapered artery under some assumptions. The resultant observations are summarized:

- As the height of the stenosis is increasing the obstruction to the flow of blood is increasing.
- Diverging tapered artery is increasing the obstruction to the flow.
- The increment in the Womersley number decreases the blood velocity.
- The axial velocity are increasing function of time.
- The velocity is a decreasing function of relaxation time $\lambda$ and retardation time $\lambda_r$.

It is observed from the comparison between the fluid models that the peak value of the velocity appears in middle of the artery (symmetry axis) for the Oldroyd-B and second grade fluids, while for Maxwell fluid the peak velocity appears near the artery wall.

The use of the VO fractional derivative in fluid models is giving more realistic results than usual derivative or CO fractional derivative.

The modeling and simulation of the previously mentioned phenomena is expected to be very useful in predicting the behavior of physiological parameters in the diagnosis of various arterial diseases.

## Nomenclature

$\mathbf{A}$ – Rivlin-Ericksen tensor, ($= \mathbf{L} + \mathbf{L}^T$), [$s^{-1}$]
$\vec{b}$ – body accelerations, [$N = kgms^{-2}$]
$D_t^{\alpha}$ – fractional time-derivatives in Caputo's sense, [–]

$d$ – location of the stenosis, [m]
$f_p$ – heart pulse frequency, [Hz = $s^{-1}$]
$k_s$ – steady-state part of the pressure gradient, [$Pam^{-1}$]
$k_\phi$ – amplitude of the oscillatory part, [$Pam^{-1}$]
$n$ – shape of the stenosis, [–]
$\mathbf{L}$ – velocity gradient, (= $\nabla\vec{V}$ ), [$s^{-1}$]
$L_0$ – stenosis length, [m]
$p$ – pressure, [Pa]
$\partial p/\partial z$ – pressure gradient, [Pa·$m^{-1}$]
$R(z)$ – radius of the tube, [m]
S – extra-shear stress tensor, [Pa]
$t$ – time, [s]
$\mathbf{T}$ – Cauchy stress tensor, [Pa]
$\vec{V}$ – velocity vector, [$ms^{-1}$]
$x$ – space, [m]

*Greek symbols*

$\overline{\alpha}$ – Womersley number, [= $R_0(\omega\rho/\mu)^{1/2}$], [–]
$\alpha(x,t)$ – the VO of the fractional derivative, [–]
$\Gamma(\bullet)$ – gamma function, [–]
$\gamma$ – defined constant (= $L_0/L_1$), [–]
$\zeta$ – tapering parameter (= tan $\phi$), [–]
$\epsilon$ – maximum height of the stenosis, [m]
$\lambda$, $\lambda_r$ – relaxation and retardation times, [–]
$\mu$ – dynamic viscosity, [Pa·s]
$\rho$ – density of the fluid, [$kgm^{-3}$]
$\omega_p$ – heart angular frequency, [Hz = $rads^{-1}$]
$\phi$ – tapering angle, [rad]
$\tau_{RZ}$ shear stress tensor acting on r-plane toward z-direction, [Pa]

*Abbreviations*

CO – constant-order
VO – variable-order

## References

[1] Oldroyd, J. G., On the Formulation of Rheological Equations of State, *The Royal Society, 200* (1950), 1063, pp. 523-541
[2] Oldroyd, J. G., The Motion of an Elastico-Viscous Liquid Contained between Coaxial Cylinders. I, *The Quarterly Journal of Mechanics and Applied Mathematics, 4* (1951), 3, pp. 271-282
[3] Rajagopal, K. R., Bhatnagar, R. K., Exact Solutions for some Simple Flows of an Oldroyd-B Fluid, *Acta Mechanica, 113* (1995), 1, pp. 233-239
[4] Pontrelli, G., Bhatnagar, R. K., Flow of a Viscoelastic Fluid between Two Rotating Circular Cylinders Subject to Suction or Injection, *International Journal for Numerical Methods in Fluids, 24* (1997), 3, pp. 337-349
[5] Hayat, T., *et al*., Some Unsteady Unidirectional Flows of a Non-Newtonian Fluid, *International Journal of Engineering Science, 38* (2000), 3, pp. 337-345
[6] Hayat, T., *et al*., Exact Solutions of Flow Problems of an Oldroyd-B Fluid, *Applied Mathematics and Computation, 151* (2004), 1, pp. 105-119
[7] Shahid, N., *et al*., Exact Solution for Motion of an Oldroyd-B Fluid over an Infinite Flat Plate that Applies an Oscillating Shear Stress to the Fluid, *Boundary Value Problems, 2012* (2012), 1, pp. 1-19
[8] Song, D. Y., Jiang, T. Q., Study on the Constitutive Equation with Fractional Derivative for the Viscoelastic Fluids – Modified Jeffreys Model and its Application, *Rheologica Acta, 37* (1998), 5, pp. 512-517
[9] Hilfer, R., *Applications of Fractional Calculus in Physics*, World Scientific Publishing Co., Singapore, 2000
[10] Podlubny, I., *Fractional Differential Equations*, Academic Press, San Diego, Cal., USA, 1999
[11] Qi, H. T., Xu, M. Y., Unsteady Flow of Viscoelastic Fluid with Fractional Maxwell Model in a Channel, *Mechanics Research Communications, 34* (2007), 2, pp. 210-212
[12] Tong, D. K., *et al*., Unsteady Helical Flows of a Generalized Oldroyd-B Fluid, *Journal of Non-Newtonian Fluid Mechanics, 156* (2009), 1-2, pp. 75-83
[13] Qi, H. T., Xu, M. Y., Some Unsteady Unidirectional Flows of a Generalized Oldroyd-B Fluid with Fractional Derivative, *Applied Mathematical Modelling, 33* (2009), 11, pp. 4184-4191
[14] Liua, Y., *et al*., Unsteady MHD Couette Flow of a Generalized Oldroyd-B Fluid with Fractional Derivative, *Computers and Mathematics with Applications, 61* (2011), 2, pp. 443-450
[15] Khandelwal, K., Mathur, V., Exact Solutions for an Unsteady Flow of Viscoelastic Fluid in Cylindrical Domains Using the Fractional Maxwell Model, *International Journal of Applied and Computational Mathematics, 1* (2015), 1, pp. 143-156
[16] Hristov, J., Approximate Solutions to Time-Fractional Models by Integral Balance Approach, in: *Fractional Dynamics*, Chapter 5, (Eds. C. Cattani, H. M. Srivastava, X.-J. Yang), De Gruyter Open, Warsaw, 2015, pp. 78-109
[17] Hristov J., Diffusion Models with Weakly Singular Kernels in the Fading Memories: How the Integral-Balance Method can be Applied?, *Thermal Science, 19* (2015), 13, pp. 947-957

[18] Samko, S. G., Ross, B., Integration and Differentiation to a Variable Fractional Order, *Integral Transforms and Special Functions, 1* (1993), 4, pp. 277-300
[19] Ross, B., Samko, S. G., Fractional Integration Operator of Variable Order in the Holder Space Hλ(x), *International Journal of Mathematics and Mathematical Sciences, 18* (1995), 4, pp. 777-788
[20] Coimbra, C. F. M., Mechanics with Variable-Order Differential Operators, *Annalen der Physik, 12* (2003), 11-12, pp. 692-703
[21] Ingman, D., Suzdalnitsky, J., Application of Differential Operator with Servo-Order Function in Model of Viscoelastic Deformation Process, *Journal of Engineering Mechanics, 131* (2005), 7, pp. 763-767
[22] Pedro, H. T. C., *et al*., Variable Order Modeling of Diffusive-Convective Effects on the Oscillatory Flow Past a Sphere, *Journal of Vibration and Control, 14* (2008), 9-10, pp. 1659-1672
[23] Lim, S. C., Teo, L. P., Sample Path Properties of Fractional Riesz-Bessel Field of Variable Order, *Journal of Mathematical Physics, 49* (2008), 1, 013509
[24] Yuste, S. B., Acedo, L., An Explicit Finite Difference Method and a New Von Neumann-Type Stability Analysis for Fractional Diffusion Equations, *SIAM Journal on Numerical Analysis, 42* (2005), 5, pp. 1862-1874
[25] Sun, H., *et al*., Variable-Order Fractional Differential Operators in Anomalous Diffusion Modeling, *Physica A: Statistical Mechanics and its Applications, 388* (2009), 21, pp. 4586-4592
[26] Sun, H. *et al*., A Comparative Study of Constant-Order and Variable-Order Fractional Models in Char- acterizing Memory Property of Systems, *The European Physical Journal Special Topics, 193* (2011), Apr., pp. 185-192
[27] Zhuang, P., *et al*., Numerical Methods for the Variable-Order Fractional Advection-Diffusion Equation with a Nonlinear Source Term, *SIAM Journal on Numerical Analysis, 47* (2009), 3, pp. 1760-1781
[28] Lin, R., *et al*., Stability and Convergence of a New Explicit Finite-Difference Approximation for the Fariable-Order Nonlinear Fractional Diffusion Equation, *Applied Mathematics and Computation, 212* (2009), 2, pp. 435-445
[29] Sun, H., *et al*., Finite Difference Schemes for Variable-Order Time Fractional Diffusion Equation, *International Journal of Bifurcation and Chaos, 22* (2012), 4, 1250095
[30] Akbar, N. S., *et al*., Nano Fluid Flow in Tapering Stenosed Arteries with Permeable Walls, *International Journal of Thermal Sciences, 85* (2014), Nov., pp. 54-61
[31] Srivastava, V. P., Mishra, S., Non-Newtonian Arterial Blood Flow through an Overlapping Stenosis, *Applications and Applied Mathematics: An International Journal, 5* (2010), 1, pp. 225-238
[32] Bakhti, H., Azrar, L., Steady Flow of Couple-Stress Fluid in Constricted Tapered Artery: Effects of Transverse Magnetic Field, Moving Catheter, and Slip Velocity, *The Royal Society, 2016* (2016), ID 9289684
[33] Bertolotti, C., *et al*., Numerical and Experimental Models of Post-Operative Realistic Flows in Stenosed Coronary Bypasses, *Journal of Biomechanics, 34* (2001), 8, pp. 1049-1064
[34] Kamenskiy, A. V., *et al*., *In Vivo* Three-Dimensional Blood Velocity Profile Shapes in the Human Common, Internal, and External Carotid Arteries, *Journal of Vascular Surgery, 54* (2011), 4, pp. 1011-1020

Paper submitted: April 21, 2016
Paper revised: May 20, 2016
Paper accepted: June 10, 2016